Key Engineering Materials
ISSN: 1662-9795, Vol. 883, pp 294-302
doi:10.4028/www.scientific.net/KEM.883.294

Submitted: 2020-10-21
Revised: 2020-11-23
Accepted: 2020-12-07
Online: 2021-04-27

Fracture Characterisation by Butterfly-Tests and Damage Modelling of Advanced High Strength Steels

Bernd-Arno Behrens, Kai Brunotte, Hendrik Wester, Matthäus Dykiert*

Institute of Forming Technology and Machines (IFUM), Leibniz Universität Hannover
An der Universität 2, 30823 Garbsen, Germany

dykiert@ifum.uni-hannover.de*

Keywords: Fracture Characterisation, Forming Limit, Damage Modelling, Butterfly-Tests, AHSS, CP800, DP1000

Abstract. Advanced High Strength Steels (AHSS) are widely used in today's automotive structures for lightweight design purposes. FE simulation is commonly used for the design of forming processes in automotive industry. Therefore, besides the description of the plastic flow behaviour, also the definition of forming limits in order to efficiently exploit the forming potential of a material is required. AHSS are prone for crack appearances without prior indication by thinning, like exemplary shear fracture on tight radii and edge-fracture, which can not be predicted by conventional Forming Limit Curve (FLC). Stress based damage models are able to do this. However, the parameterisation of such models has not yet been standardised. In this study a butterfly specimen geometry, which was developed at the Institute for Forming Technology and Machines (IFUM), was used for a stress state dependent fracture characterisation. The fracture behaviour of two AHSS, CP800 and DP1000, at varied stress states between pure shear and uniaxial loading was characterised by an experimental-numerical approach. For variation of the stress state, the specimen orientation relative to the force direction of the uniaxial testing machine was orientated at different angles. In this way, the relevant displacement until fracture initiation was determined experimentally. Subsequently, the experimental tests have been numerically reproduced giving information about the strain and stress evolution in the crack impact area of the specimen for the experimentally identified fracture initiation. With the help of this testing procedure, two different stress-based damage models, Modified Mohr-Coulomb (MMC) and CrachFEM, were parameterised and compared.

Introduction

Advanced High Strength Steels (AHSS) are commonly used in modern car body design in order to reduce mass and improve safety requirements. AHSS combine high strength with relatively good ductility by means of a carefully adjusted multiphase microstructure, which consists of soft and ductile matrix (e. g. ferrit) as well as additional hard constituents (e. g. martensit). Higher strength is usually accompanied by a reduction in formability. In this context, it is especially important to exhaust the full formability potential of AHSS. As a matter of fact, numerical methods are used in this context to design and optimise complex sheet metal forming processes regarding material distribution and forming capacity. Different approaches for numerical sheet metal forming simulation are available to describe the formability or forming limits on the macroscopic component scale. The forming limit curve, also called FLC, is commonly used to describe the onset of localised necking in the relationship of the principal strains. An FLC is only valid for linear strain paths in the range between uniaxial and equibiaxial tension and is for this reason not able to predict shear fracture, edge-fracture or fracture induced by complex loading histories resulting in a nonlinear strain path. The damage behaviour of AHSS is affected by the multiphase structures, in which morphological irregularities and hardness differences lead to high stress gradients. This results in a propensity for different crack appearances, without prior indication by thinning, like exemplary shear fracture on tight radii and edge-fracture, which all can not be predicted by an FLC. These challenges in numerical damage prediction are exemplary demonstrated in [1] and confirmed in [2]. Moreover, the fracture behaviour of AHSS compared to conventional steels, results in a propensity for shear failure as opposed to ductile failure caused by thinning for example during automotive panel stamping.

The disadvantages of an FLC can be overcome by using extended model approaches. For example, coupled micromechanical damage models and uncoupled phenomenological damage models can be used. The parameterisation of uncoupled models proves to be significantly simpler and can be carried out based on some experimental data points in dependence of the stress state. By means of these so-called stress state dependent models, the damage evolution is phenomenologically described in dependence on the stress triaxiality η defined by the ratio of the Mises equivalent stress to the mean principal stress, and the normalized Lode angle $\bar{\theta}$, which corresponds to a function of the third deviatoric stress invariant [3].

The damage accumulation of non-linear loading paths can be considered due to an incremental contribution of the equivalent plastic strain. Model approaches such as Xue-Wierzbicki [4], CrachFEM [5], Modified Mohr-Coulomb (MMC) [6] have shown good results for damage representation of high strength steels, for example for a TRIP690 steel in [1] and a DP600 steel in [2]. In order to parametrise these kind of models, the fracture behaviour has to be identified within different tests under consideration of various stress states. However, tests for parametrisation of these kind of models are currently not standardised, resulting in a variety of tests for their parameterisation. In a comprehensive study, Behrens et al. compared different experimental methods and discussed the advantages and disadvantages of common tests [7]. In this study and in a further application in [2], a methodology with a special butterfly specimen geometry, which was developed at the IFUM [8], showed good applicability for a DP600 steel. This approach is therefore chosen to be applied in this work for the investigation of the damage behaviour of two other AHSS, a dual-phase DP1000 and a complex-phase CP800 sheet metal material. In this way, two damage models CrachFEM and MMC are parameterised for the two AHSS.

Materials

The investigations were carried out with a dual-phase steel DP1000 (1.5 mm) and a complex-phase steel CP800 (1.6 mm), which were produced by voestalpine Stahl GmbH. The microstructure of the DP1000 steel is composed of a ferritic matrix with accumulations of martensite. In addition to these microstructure phases, the CP800 also contains a bainitic phase. The chemical compositions of the investigated AHSS are presented in Table 1.

Table 1. Chemical composition of CP800 and DP1000 in %

	C	Si	Mn	P	S	Al	Cr+Mo	Ti+Nb	B	Cu
DP1000	0.23	1.00	2.90	0.050	0.010	0.01 - 1.0	1.40	0.15	0.005	0.20
CP800	0.18	1.00	2.50	0.50	0.010	0.01 - 1.0	1.00	0.15	0.005	0.20

Characterisation of Flow Behaviour

The parametrisation of the damage behaviour is performed by an experimental-numerical approach in the following sections. For the FE simulations to be carried out, it is therefore necessary to describe the plastic material behaviour in advance. Therefore, tensile-tests at isothermal, quasi-static conditions at room temperature were conducted with a standardised A80 sample. Three different rolling directions were considered in order to measure besides the anisotropic plastic hardening behaviour: 0° (rolling direction, RD), 90° (transversal direction, TD) and 45°. The tests were performed in displacement control with a nominal strain rate of 0.0025 s^{-1} on a uniaxial testing machine S100/ZD by Dynamess. The change in width was measured by means of an extensometer. Five repeat tests were acquired for each direction. The mechanical properties determined in this way for the two AHSS are summarised in Table 2, whereby clear differences in strength and formability are evident. Both steels have a relatively high strain hardening exponent (n-value) and thus a high resistance to local necking.

Table 2. Mechanical properties of investigated cold-rolled steels DP1000 and CP800 determined by quasi-static, isothermal uniaxial tensile tests performed at 20 °C

	Thickness [mm]	σ_{YS} [MPa]	σ_{UTS} [MPa]	n [-]	ε_{UTS} [%]	ε_{Break} [%]
DP1000	1.6	757.3	1043.3	0.08	7.4	12.0
CP800	1.5	631.4	809.0	0.11	9.5	16.4

Based on the anisotropy values determined by tensile tests for each of the three rolling directions, the coefficients for the anisotropic yield function Hill48 were calculated, see Table 3.

Table 3. Anisotropy coefficients and Hill48 yield function coefficients

	r_0	r_{45}	r_{90}	F	G	H	N	L	M
DP1000	0.904	1.040	1.068	0.445	0.525	0.475	1.494	1.5	1.5
CP800	0.884	1.094	0.949	0.495	0.531	0.469	1.634	1.5	1.5

The force-displacement developments of the uniaxial tensile tests in RD are each shown for all repeats in Fig. 1 a. In addition, equibiaxial bulge tests were carried out with the two AHSS in order to extend the uniaxial flow curves beyond the uniform elongation and experimentally increase the accuracy for subsequent analytic extrapolations. The transformation from biaxial to uniaxial stress data was performed with the help of the approach on plastic work according to Sigvant et al. [9], which has proven its quality over the past years. Subsequently, the combined experimental flow curves were extrapolated by analytical approaches, wherby the approach by Hockett-Sherby showed good accuracy for both materials as depicted in Figure 1b. The corresponding equation and parameters are given in Table 4.

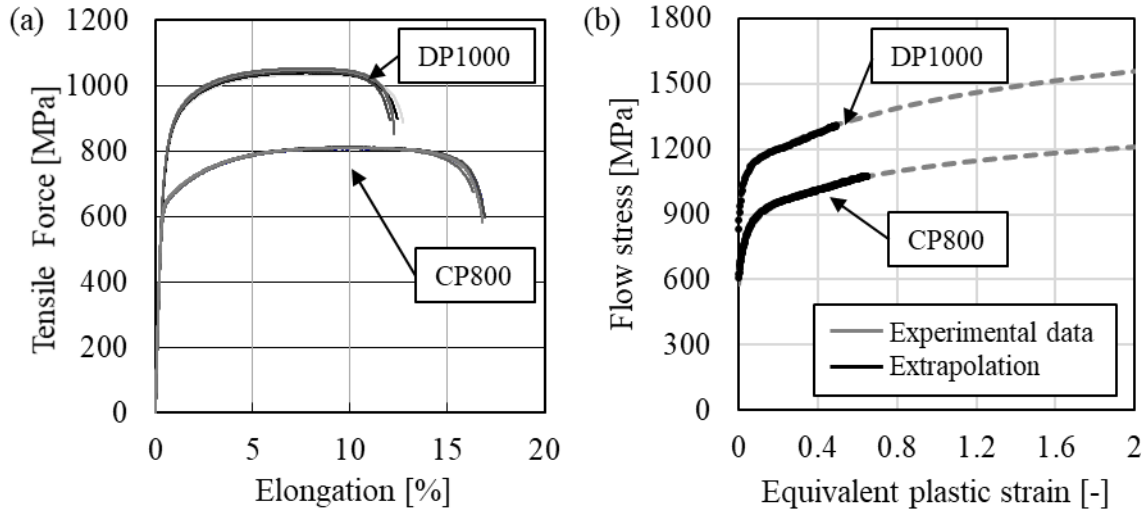

Figure 1. Results of tensile tests for DP1000 and CP800 in RD: Force-displacement developments (a) and uniaxial flow curves extended by bulge tests and extrapolated by (b) in RD

Table 4. Parameter for flow curve extrapolation (Hockett-Sherby approach)

	Equation	a	b	c	d
DP1000	$k_f = a - (a-b)e^{c\bar{\varepsilon}^d}$	0.0001282	795.9	0.575	0.209
CP800		4.96 E-05	502.5	0.823	0.170

Characterisation of Fracture Behaviour

Testing Procedure. In order to investigate the fracture behaviour of the two AHSS, a butterfly specimen, which has been developed at the IFUM recently [8], was used in this study (Fig. 2 a). The specific feature of this sample is the investigation area with an adapted thickness reduction. In this way, the specimen has been optimised for the investigation of the fracture behaviour in such a way that the specimen can be loaded under different angles (here defined as alpha). Thereby the fracture initiates irrespectively of the angle in the centre of the investigation area, where a specific stress state for the corresponding angle prevails. For manufacturing the sample, the outer contour is first removed from the sheet by wire erosion and then the thickness reduction of 25 % of the initial sheet thickness is carried out by CNC-machining on each specimen half, whereby roughness values of $R_a < 0.8$ and $R_z < 6.3$ are ensured.

A special testing device, according the Arcan Principle [10], is used to perform the tests with the IFUM Butterfly-Specimen, which allows the sample to be rotated relatively to the load direction by adjusting the specimen holders (Fig. 2 b). The sample is clamped in the two-part holders with the help of fastening plates, which can be fixed at different angles in the fixtures by means of fitting pins. With this device, tests are carried out for five different loading angles, which result in a stress range from pure shear to tension. Tests were performed under quasi-static conditions with a velocity of 0.02 mm/s until a fracture occurs. An optical measuring system Aramis (by GOM GmbH) is also used to measure strain in the investigation area of the sample and the movement of the attached fastening plates in order to accurately record the relative translation of the two halves of the specimen holder. Tests with loading angles ranging from -3°, 12.5°, 28°, 43.5° and 59° were carried out with both materials.

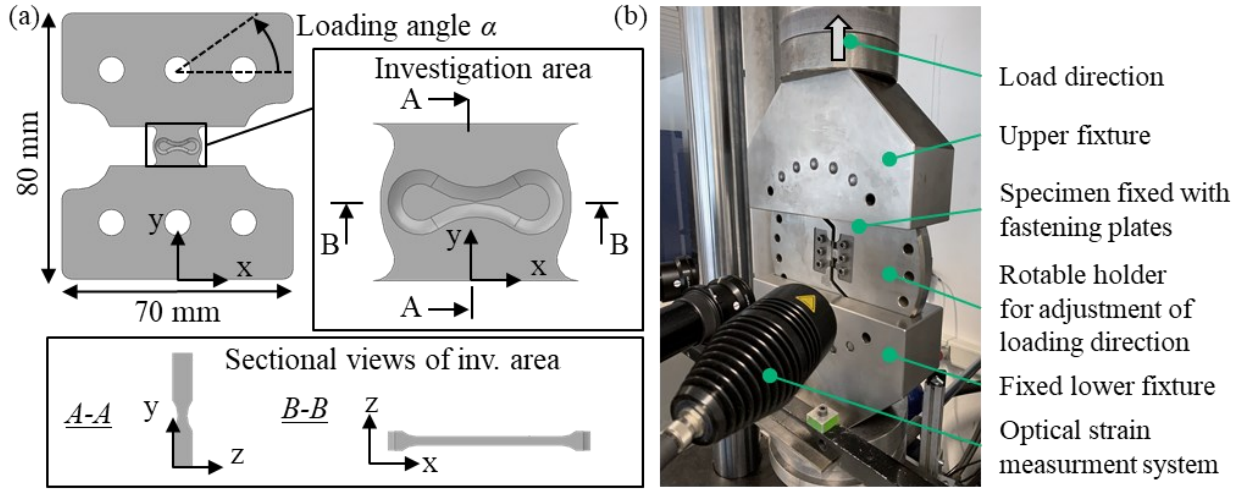

Figure 2. (a) IFUM-Butterfly specimen with investigation area of reduced thickness, (b) testing device for variation of the specimen orientation regarding the loading direction

Experimental-Numerical Approach. For the parameterisation of stress based models, it is required to identify the stress history at the location of crack initiation. Stress evolution at this position must therefore be calculated numerically. So an experimental–numerical approach is used for the fracture characterisation. The fracture initiation and the corresponding translation of the tools (fracture displacement $u_{f,xy}$) is determined experimentally with the help of the optical measurement system. Subsequently, the tests are numerically reproduced. The point of fracture initiation is defined by using the experimentally determined mean value of the fracture displacement as a boundary condition. Thereby, the corresponding stress evolution and equivalent plastic strain are evaluated for the critical element in the centre of the investigation zone, which is assumed to be the most deformed element.

In the numerical model, the specimen is reproduced with the adjacent tool surfaces of the specimen holder and the fastening plates to which a surface pressure converted from the screw force is applied

(Fig. 3). The lower half of the tool is fixed, and the experimentally measured mean fracture displacement $u_{f,xy}$ is applied to the other upper specimen holder in the particular loading angle. This displacement is the resulting vector in x- and y-direction of the two tool halves. Simulations of each experiment are carried out using the FE-Software Abaqus with an implicit solver. Continuum eight-node linear elements with reduced integration (C3D8R) of a size of 0.1 mm are used for an adequate discretization of the specimen and the tools are modelled as elastic solids. The elastic material behaviour was described with an elastic modulus of 210 GPa and a Poisson ratio of 0.3. The plastic properties were defined in accordance with the material data listed in the previous section.

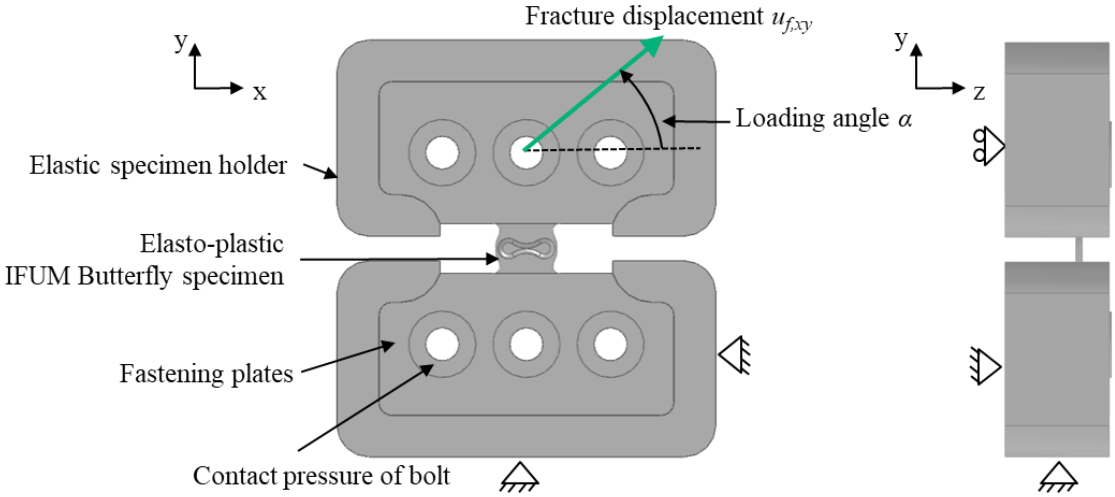

Figure 3. Numerical model for FE-simulation of IFUM-Butterfly tests

Experimental-numerical Results. The fracture initiated for both AHSS and all angles in the centre of the investigation zone. In Fig. 4, the experimental fracture occurrence is exemplary shown for CP800 and two loading angles. The fracture initiation could be well identified with the help of the optical measuring system and could also be confirmed by the drop in the measured tensile force of the testing machine.

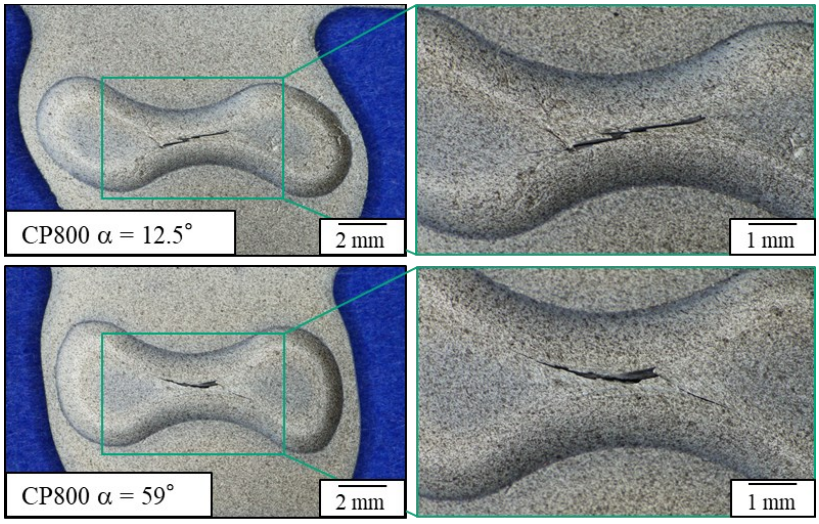

Figure 4. Fracture occurrence for exemplary tests at different angles with CP800.

Figure 5a shows a comparison of the experimental fracture occurrence and the numerical strain distribution for a representative test. This figure only serves as a qualitative comparison, as there are different deformation conditions in both cases. In the simulation the onset of fracture is shown and experimentally the test was carried out until the presence of a significant crack appearance. For the onset of fracture, the equivalent plastic strain determined by the optical strain measurement system and the FE-simulation are depicted in Fig. 5 b. The measured strain distribution is well-replicated by the numerical model.

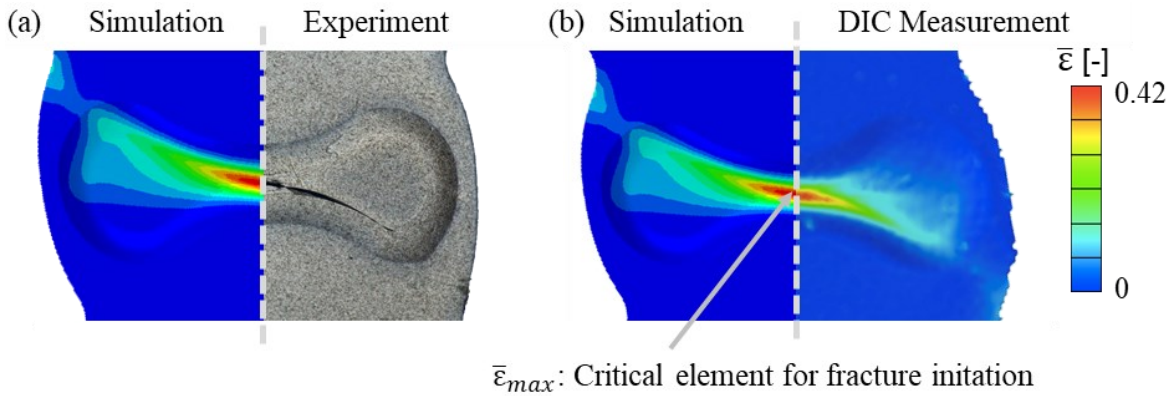

Figure 5. Comparison of numerical results of equivalent plastic strain distribution with experimental fracture occurrence (a) and optical strain measurement at fracture initiation (b) for DP1000, α = 59°.

In Figure 6a, the force-displacement curves from numerical simulation and the experiment are compared exemplary for the DP1000 and three different loading angles until the fracture initiation. Due to a good agreement, it can be assumed that the material model being used reproduces the plastic behaviour with sufficient accuracy. Comparable results were also achieved with the CP800. Smaller discrepancies between experimental and numerical results, which can be seen at the beginning of the test, are probably caused by differences in the stiffness assumptions of the machine and experimental set-up. Based on the strain path developments shown in Figure 6b, which were recorded up to the crack by means of optical measurement, the range of application of the butterfly tests outside the scope of an FLC can be demonstrated. The optical measurement using DIC was more complicated with the more ductile material CP800 due to facet failures caused by high shear deformations. This resulted in a gap in the relevant centre of the investigation zone, where the strain could not be evaluated. The strain distributions for both materials were therefore numerically evaluated.

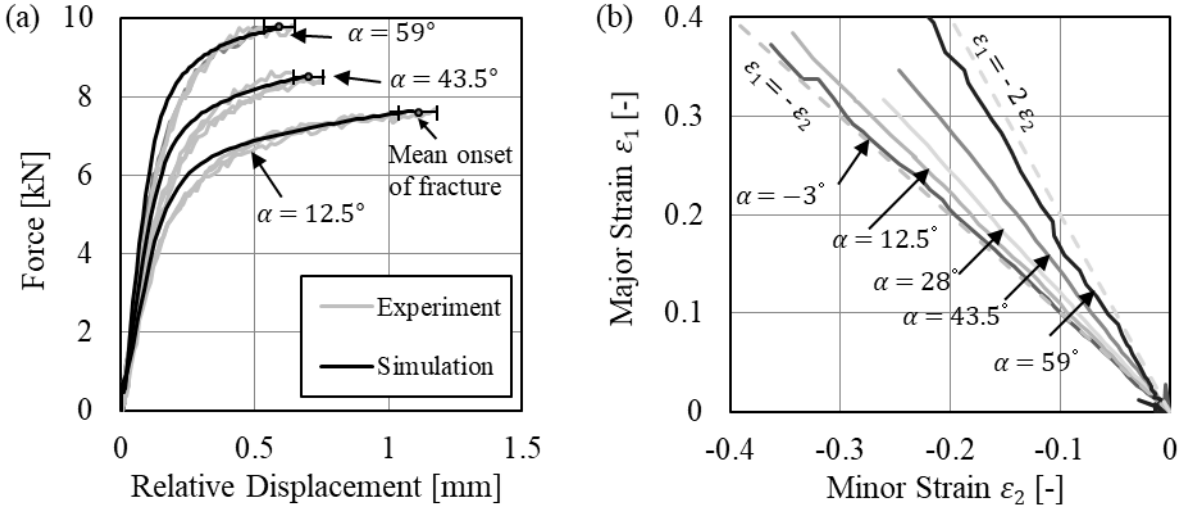

Figure 6. Results for DP1000: (a) Experimental and numerical force-displacement evolution until fracture, (b) Optically determined strain paths in the centre of the specimen.

In the numerical simulation, the most highly deformed element was identified for the experimentally determined onset of fracture. It is assumed that fracture initiation takes place at this so-called critical element. The stress evolution for the critical element at each loading angle until fracture is depicted as a black line in Figure 7a. Stress states of triaxiality of 0 to 0.33 were evaluated based on the performed tests with different loading angles from -3° to 59°, which corresponds to stress conditions of pure shear and uniaxial tension. The stress triaxiality is not constant during the deformation, but increases initially at each loading angle. However, for the parameterisation of stress state dependent damage models characteristic stress value are required for each test respectively the fracture strain determined in the specific test. For this reason, a characteristic averaged value for the stress evolution

was determined using the centre of area. It can be seen in Figure 7b that the stress evolutions correspond to the plane stress state for the investigated loading angles from -3° to 59°. The characteristic damage values are marked with a grey triangle and were subsequently used to parameterise the damage model. Lode angles for these values range approximately between 0 to 1

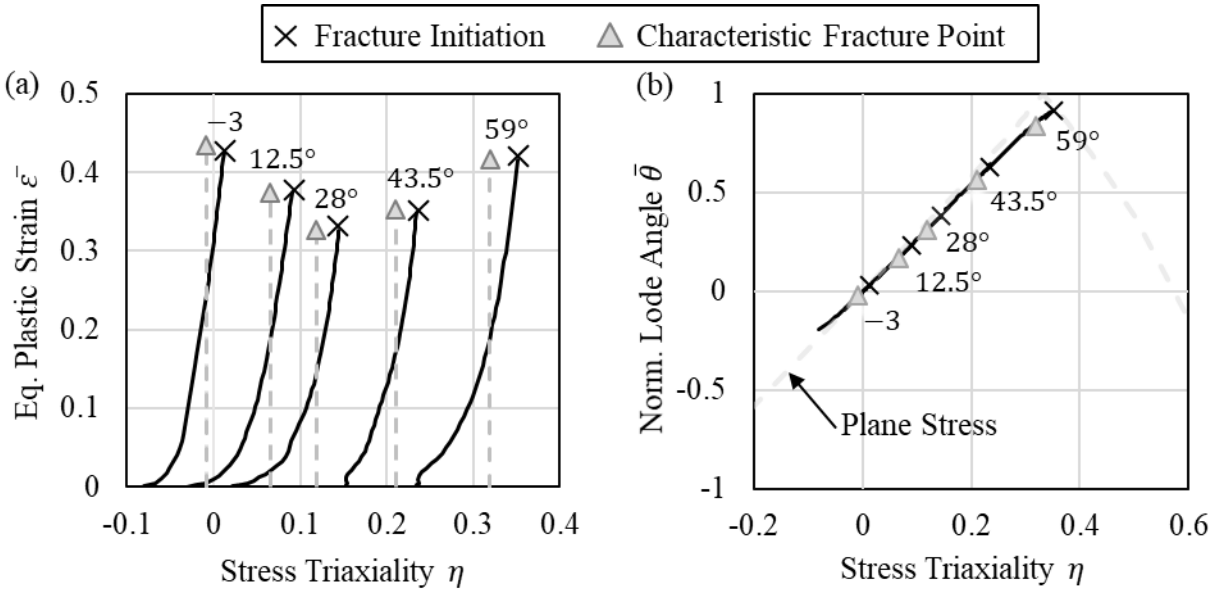

Figure 7: Stress evolution at critical element exemplary for DP1000 in dependence on the loading angle: (a) Equivalent plastic strain against stress triaxiality (black line) and averaged stress triaxiality (grey line), (b) Norm. Lode angle against stress triaxiality

Damage Modelling

Using results of the presented methodology and the determined characteristic fracture points, two different damage models, MMC and CrachFEM, were parameterised. For parametrisation of the damage models, the equivalent strain to fracture from the bulge test (see section Characterisation of Flow Behaviour) for a stress triaxiality of 0.67 was additionally used. The parameters of the models were calculated according to the method of the least square error and are provided in Table 4.

Table 4. Parameters of MMC and CrachFEM damage models for DP1000 and CP800

	MMC				CrachFEM			
	A / C_2	C_1	C_3	n	k_S	ε^+	ε^-	f
DP1000	2.00	0.190	1.030	0.221	0.03	0.231	1.200	0.296
CP800	1.90	0.065	0.990	0.160	0.02	0.733	1.518	0.149

For plane stress conditions, the fracture curves are depicted in Figure 8 for the two sheet metals. The two models only exhibit small differences in areas between pure shear and uniaxial tension ($0 < \eta < 0.33$), more precisely where the characteristic fracture points are provided that are used to parameterize the models. The areas between uniaxial pressure and pure shear ($-0.33 < \eta < 0$) and around the plane strain region ($0.5 < \eta < 0.6$) show larger differences. Comparing the formability of the two materials, the CP800 has nearly twice the forming capacity of the DP1000 in areas of uniaxial tension to plane strain between $0.2 < \eta < 0.6$. In the region of shear ($0 < \eta < 0.2$) this difference is not as pronounced amounting approximately 25%.

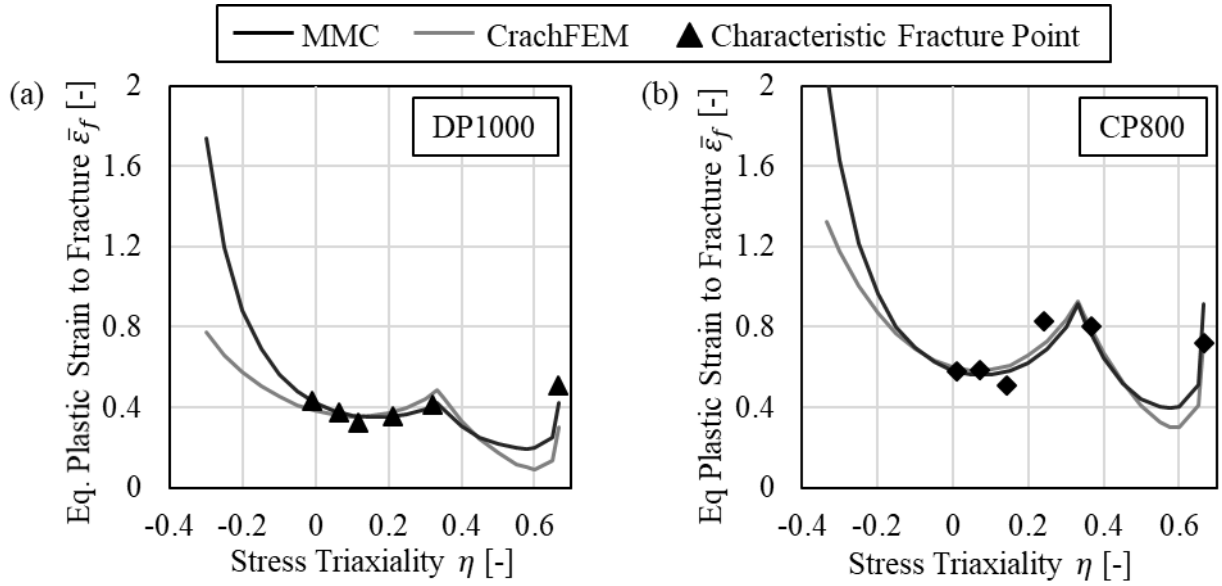

Figure 8: Fracture curves for MMC and CrachFEM damage models for plane stress conditions for DP1000 (a) and CP800 (b).

Apart from the presented fracture curves, which are of relevance for plane stress states, all possible stress states in a forming process can be represented in terms of a fracture surface. For this purpose, in addition to the stress triaxiality, the normalised Lode angle is taken into account. In order to illustrate exemplary such a failure surface, the MMC damage model for DP1000 is depicted in Figure 9. Consequently, these failure curves or surfaces can be implemented in the FE environment to reproduce the damage evolution of forming processes. A further validation of the parametrised fracture models based on experimental tests is necessary and planned in the near future in order to assess the quality and evaluate achievable improvements.

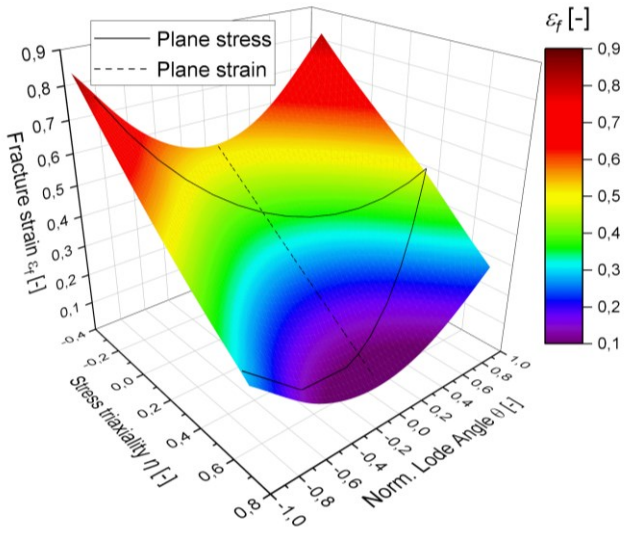

Figure 9: Fracture surface in dependence on stress triaxiality and norm. Lode angle for MMC damage model (DP1000)

Summary

In this contribution, the stress state dependent fracture behaviour of two AHSS, DP100 and CP800, was characterised by means of so-called IFUM-Butterfly tests. The tests were performed in the range of pure shear and uniaxial stress and were performed for all stress states with an identical specimen geometry. To vary the stress state, the specimen orientation to the tensile direction of the testing machine was changed with the help of a testing device based on the Arcan principle. Using an

experimental-numerical approach, the tests were evaluated. The displacement of the grips for the onset of fracture was determined experimentally and used for the numerical reproduction of the test. Hereby, corresponding relevant fracture data in terms of the equivalent plastic strain, the stress triaxiality and the normalised Lode angle were determined by numerical simulation for the onset of fracture. The tests included a range of stress triaxiality between 0 and -0.33 and norm. Lode angle between 0 and 1. In this manner, two different stress state dependent damage models, CrachFEM and MMC, were parameterised for the two AHSS. Both models were able to reproduce the data sets well. The two models exhibit differences in uniaxial pressure and pure shear ($0.33 < \eta < 0$) and around the plane strain region ($0.5 < \eta < 0.6$). In the near future, an experimental-numerical validation considering a deep drawing process will be performed in order to assess the quality of the parametrised damage models. Furthermore, a new testing device is under development in this project, which is able to adjust the loading angle in order to achieve constant stress conditions at the location of onset of fracture.

Acknowledgement

The authors are much obliged to the DFG (Deutsche Forschungsgemeinschaft, German Research Foundation) for the financial support of project 405334714. Furthermore, the authors would like to thank voestalpine Stahl GmbH for the provision of the materials under investigation.

References

[1] Y. Li, M. Luo, J. Gerlach, T. Wierzbicki, Prediction of shear-induced fracture in sheet metal forming, Journal of Materials Processing Technology 210 (2010) 1858–1869.

[2] B.-A. Behrens, C. Bonk, I. Peshekhodov, On modelling of shear fracture in deep drawing of a high-strength dual-phase sheet steel, Journal of Physics: Conference Series 896 (2017) 12125.

[3] Y. Bai, T. Wierzbicki, A new model of metal plasticity and fracture with pressure and Lode dependence, Int. J. of Plasticity 24/6, (2008), 1071-1096.

[4] T. Wierzbicki, L. Xue, On the effect of the third invariant of the stress deviator on ductile fracture, Impact and Crashworthiness Lab Report 136, Int J of Fract, (2005).

[5] H. Dell, H. Gese, G. Oberhofer, CrachFem - A Comprehensive Approach for The Prediction Of Sheet Metal Failure, AIP Conf. Proc. 908 (2007) 165-179.

[6] A. M. Beese, Luo, M., Y. Li, Y. Bai, T. Wierzbicki, Partially coupled anisotropic fracture model for aluminum sheets, Engineering Fracture Mechanics 77 (2010) 1128–1152.

[7] I. Peshekhodov, M. Dykiert, M. Vucetic, B.-A. Behrens, Evaluation of common tests for fracture characterisation of advanced high-strength sheet steels with the help of the FEA, IOP Conf Ser: Mat Sci Eng 159 (2016) 12014.

[8] I. Peshekhodov, S. Jiang, M. Vucetic, A. Bouguecha, B.-A. Behrens, Experimental-numerical evaluation of a new butterfly specimen for fracture characterisation of AHSS in a wide range of stress states, IOP Conf Ser: Mat Sci and Eng 159 (2016) 12015.

[9] M. Sigvant, K. Mattiasson, H. Vegter et al., A viscous pressure bulge test for the determination of a plastic hardening curve and equibiaxial material data. Int J Mater Form 2 (2009) 235.

[10] M. Arcan, Z. Hashin, A. Voloshin, A method to produce uniform plane-stress states with applications to fiber-reinforced materials, Exp Mech 18 (1978), 141-146.